JOURNAL OF MATERIALS SCIENCE **40** (2005) 6121–6126

Effect of in-flight particle oxidation on the phase evolution of HVOF NiTiZrSiSn bulk amorphous coating

HANSHIN CHOI
Nano Material Team, Korea Institute of Industrial Technology, Incheon, 404-254, Korea

SANGYONG LEE
Division of Materials Science & Engineering, College of Engineering, Hanyang University, 17 Haengdang-dong, Seongdong-gu, Seoul 133-791, Korea

BYOUNGMOON KIM
Research Institute of Industrial Science & Technology (RIST), Hyoja-dong Nam-gu Pohang, 790-330, Korea

HYOUNGHO JO
Nano Material Team, Korea Institute of Industrial Technology, Incheon, 404-254, Korea

CHANGHEE LEE*
Division of Materials Science & Engineering, College of Engineering, Hanyang University, 17 Haengdang-dong, Seongdong-gu, Seoul 133-791, Korea
E-mail: chlee@hanyang.ac.kr

Bulk amorphous NiTiZrSiSn feedstock was sprayed using a high velocity oxy-fuel spraying process. In order to evaluate the amorphous formability in view of chemical instability, the oxygen to hydrogen gas flow rate ratio was changed at the constant total gas flow rate. Flame gas enthalpy was increased with the O_2/H_2 gas ratio. In-flight particle melting state was improved with the increase of oxidizer flow rate. Accordingly, porosity as well as unmelted particle size and density were decreased. For the amorphous phase fraction within an as-sprayed coating, it was decreased with the oxygen flow rate. From the thermal analysis and X-ray diffraction, the effects of O_2/H_2 gas ratio on the crystallization of HVOF sprayed bulk amorphous NiTiZrSiSn could be divided into two categories. One is due to the solid-state crystallization during flight along the low gas enthalpy flame. The other results from the destabilization of bulk amorphous feedstock due to the chemical composition change resulting from in-flight particle oxidation at the higher oxygen gas flow rate. Oxidation degree was different from the O2/H2 gas ratio and it had influences on the glass formability [ΔTx] and crystalline phase. Increase of oxide phase fraction was parallel to that of γ-Ni solid solution. © *2005 Springer Science + Business Media, Inc.*

1. Introduction

Amorphous materials are thought to be promising metallic materials owing to their useful engineering properties including corrosion and wear resistance [1–6]. Also, they can be used as a precursor for making nanostructured materials. Developing advanced amorphous materials has been focused on the increase of glass formability and optimization of microstructure. As a matter of fact, a great number of bulk amorphous materials have been developed and their mechanical properties are improved by making a nano-crystalline embedded amorphous matrix composite material [1, 6, 7]. From the engineering perspective, application technology for newly developed engineering materials needs to be developed. Coating technology is more effective in view of the fact that most of the degradations of structural materials result from the surface reactions. Thermal spraying technology has become a well established coating technology. Recently, it has drawn much more attentions in industrial applications as the kinetic spraying process has been commercialized. From the viewpoint of the deposition mechanism of impacting

---

*Author to whom all correspondence should be addressed.

0022-2461 © *2005 Springer Science + Business Media, Inc.*
DOI: 10.1007/s10853-005-3169-z

particles, thermal processes is primarily dependent on the flattening and solidification of a molten droplet. Kinetic spaying is dependent on the plastic deformation of a solid particle having a higher impacting velocity than a certain critical particle velocity. For the high velocity oxy-fuel spraying process, it can be assumed as an intermediate state of thermal plasmas and cold gas dynamics. The particle deposition can be controlled by the combination of thermal energy and kinetic energy of the particle at the moment of impact. That is to say, particles can attain deposition when either of the energies[thermal energy and kinetic energy] is above a certain criterion. There are a lot of parameters affecting the in-flight particle characteristics. Among them, oxygen to fuel gas flow ratio is a critical parameter for the applications of metallic feedstock materials. According to the gas mixture, the particle temperature and velocity are different. Furthermore, the particle oxidation can be different. As a result, coating properties as well as coating microstructures are affected. Amorphorization of bulk amorphous alloys depends on the cooling rate during solidification. There is also a glass transition temperature [Tx] above which the crystallization occurs. Thus, cooling rate of an individually impacted droplet should be above a certain critical cooling rate and the temperatures of both in-flight particle and solidified splat should be suppressed below Tx during the process in order to produce amorphous coating. In addition, the chemistry of bulk amorphous alloys has a critical influence on the dependence of amorphous formation on the cooling rate during solidification, which can be considered as chemical instability. This means that the so-called glass formability including critical cooling rate is different according to the chemistry. During the thermal spraying processes, the deviation from an optimized chemistry of bulk amorphous feedstock results from the vaporization and/or oxidation of in-flight particles. Accordingly, retention of amorphous phase or in-situ composite coating formation can be possible if the responses of amorphous feedstock to the process parameters are exploited. In this study, the effect of oxygen to hydrogen gas ratio on both in-flight particle oxidation and amorphous formation were investigated.

2. Experiment

A NiTiZrSiSn bulk amorphous feedstock was manufactured using an inert gas atomization. Then the powder characterizations were conducted; X-ray diffraction for phase identification, DSC for thermal properties, scanning electron microscopy for morphology, Leco inert gas fusion method for oxygen content, and laser light scattering for size distribution. Process gas mixture for HVOF process consisted of hydrogen gas as fuel gas and oxygen gas as oxidizer. In the case of the HVOF process, particle behaviors during flight are largely dependent on the flame characteristics such as flame temperature, velocity, and oxidizing power. Also, flame characteristics depend on the process parameters. In fact, total gas flow rate and oxygen to fuel gas ratio are very important to change the particle properties though there are many factors affecting the flame characteristics and in-flight particle behaviors. When it comes to the total gas flow rate effect on the particle properties, the particle velocity is increased with the increase of the total gas flow rate. This results from the increase of combustion chamber pressure. As the particle velocity is increased, the spreading and contact are enhanced due to the increased kinetic energy. Meanwhile, the particle temperature and oxidation are decreased because the residence time of in-flight particles within a flame is inversely proportional to the particle velocity and both heating and oxidation reactions are time dependent reactions. On the other hand, oxygen to fuel gas ratio has some critical influences on the flame, particle temperatures, and oxidation degree of particle. As the oxygen flow rate is increased at the constant fuel gas flow rate, flame temperature is increased to reach a maximum one and then it is decreased. The maximum temperature is attained at the stoichiometric ratio. Before it and above it, the excess mass of process gas that does not take part in combustion needs to be heated at the certain gas enthalpy produced by combustion. In addition, the partial pressure of free oxygen molecules within a flame is increased with the increase of oxygen gas flow rate. It is the main reason for the increased particle oxidation. In this study, the total gas flow rate was fixed to 880 slm while the oxygen to hydrogen gas ratio was changed. In addition, the spraying distance was constant as shown in Table I. Through this experimental table, particle temperature flying at a different flame having a different O_2/H_2 ratio as well as free oxygen partial pressure were varied. Microstructural characterizations of the as-sprayed coatings were similar to those of the feedstock. Amorphous phase fraction of as-sprayed coating was calculated using DSC data according to ref. [8]. And oxygen content was measured using energy dispersion spectroscopy.

TABLE I Process parameters

	Working gas [SLPM]			Invariable parameters	
Designation	H_2 flow rate	O_2 flow rate	O_2/H_2 ratio		
A1	800	80	0.10	Carrier gas	12 SLPM
A2	760	120	0.15	Feed rate	60 g m^{-1}
A3	720	160	0.20	Spraying distnace	300 mm
A4	640	240	0.30		

*Stoichiometric O_2/H_2 ratio is 0.5

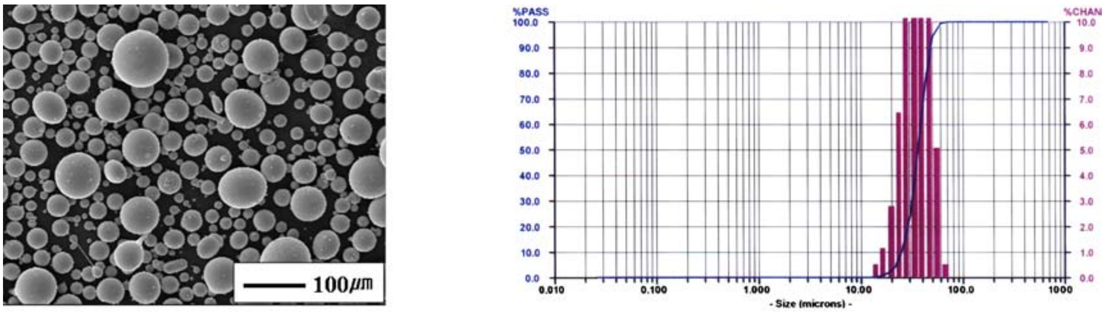

(a) Morphology

(b) Size distribution

(c) Phase composition

(d) Thermal analysis

Figure 1 Phase composition and thermal properties of starting feedstock.

3. Results

3.1. Feedstock characteristics

The chemistry of feedstock used in this study was optimized in view of glass formability. Through the calorimetry, the glass transition temperature and crystallization temperature were measured. And the glass formability(Tx−Tg=ΔTx) of as-produced feedstock was 48 °C. Through the X-ray diffraction, a broad diffuse peak without any marked crystalline peak was obtained as shown in Fig. 1a. Owing to its manufacturing method, the particle showed spherical and smooth surface morphology. When the cross section of feedstock powder was observed, it was hard to find out the inherent pores. Oxygen content of feedstock was 0.11 wt.%. Mean particle size was 37 μm; 20% of fine particles were below 30 μm while 20% of coarse particles are above 45 μm.

3.2. As-sprayed coating characteristics

According to O_2/H_2 ratio, cross sectional microstructure changes of the as-sprayed bulk amorphous coating can be seen in Fig. 2. Similar to the other thermal spraying processes, HVOF sprayed coating microstructure is largely dependent on the impacting particle energy and resulting deposition phenomena. Energy state of particle at the moment of impact could be estimated from the microstructural features according to gas mixture composition. As the O_2/H_2 ratio is increased, unmelted particle size and number density are decreased and then it disappears after the O_2/H_2 ratio of 0.2. The flattening ratio is considered to be increased with the increase of O_2/H_2 ratio from the viewpoint of splat thickness. As the total gas flow rate was constant, the increased flattening ratio might be due to the increased particle temperature that decreases the viscosity of a spreading liquid.

TABLE II Characteristics of bulk amorphous feedstock

Nominal chemistry [wt.%]	Oxygen [wt.%]	Morphology	Phase	Thermal properties	
				Tg	Tx
Ni57Ti18Zr 20Si3Sn2	0.11	Spherical	Amorphous	549	597

To identify the participating phases within a coating, energy dispersion spectroscopy was conducted on the cross section. It can be seen in Fig. 3 taken from a back scattering image of scanning electron microscopy. Pores, marked 1, results from the insufficient filling of interstices by successively overlaying droplet during spreading. Pore plays a negative role in mechanical properties and corrosion resistance. Number 2 shows an unmelted particle. It results from the insufficient thermal interaction between in-flight particles and flame jet. Unmelted particles present in the coating itself deteriorates the mechanical properties and also it promotes to form pores around it by the shadow effect. Areas showing dark gray indicated by arrows are oxides which are zirconium/zirconium and titanium complex oxides seen by energy dispersion spectroscopy.

Through the X-ray diffraction as shown in Fig. 4, the phase evolution according to gas composition can be observed. For the O_2/H_2 ratio of 0.10 and 0.15, a broad peak with a few crystalline phases such as Ni(Ti,Zr) and $Ni10(Ti,Zr)_7$ and an oxide peak could be observed. However, oxide and γ-Ni solid solution peaks were markedly enhanced with the oxygen flow rate after 0.2 O_2/H_2 ratio. Participating oxide phases were zirconium and zirconium/titanium complex oxides. Amorphous phase fraction in Fig. 5 was calculated from DSC data as following the ref.[8]. In the case of coating produced at the 0.30 O_2/H_2 ratio, a null amorphous fraction was

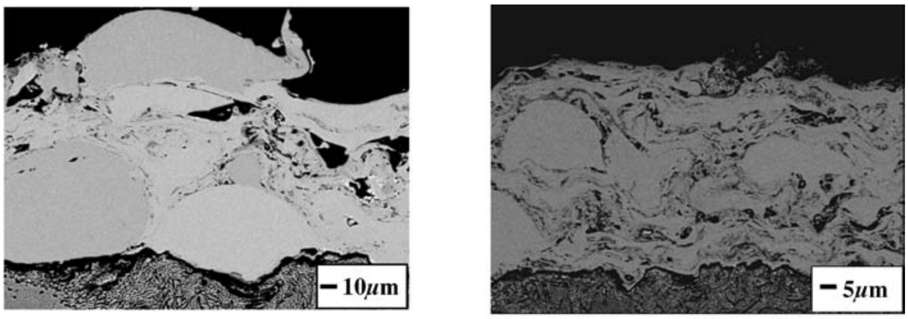

(a) 0.10 O_2/H_2 ratio (b) 0.15 O_2/H_2 ratio

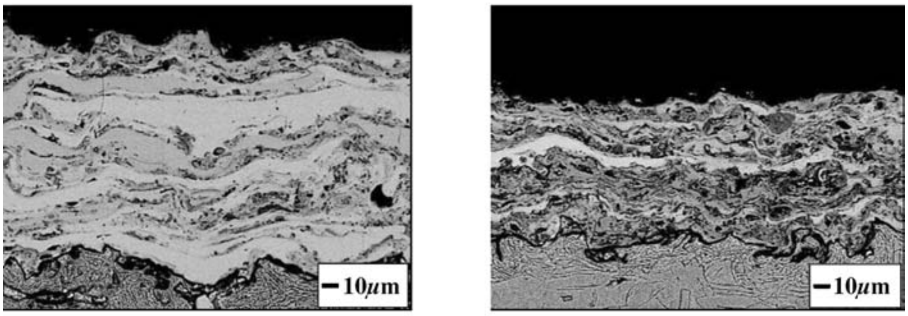

(c) 0.20 O_2/H_2 ratio (d) 0.30 O_2/H_2 ratio

Figure 2 Cross sectional morphology of as-sprayed coating according to O_2/H_2 ratio.

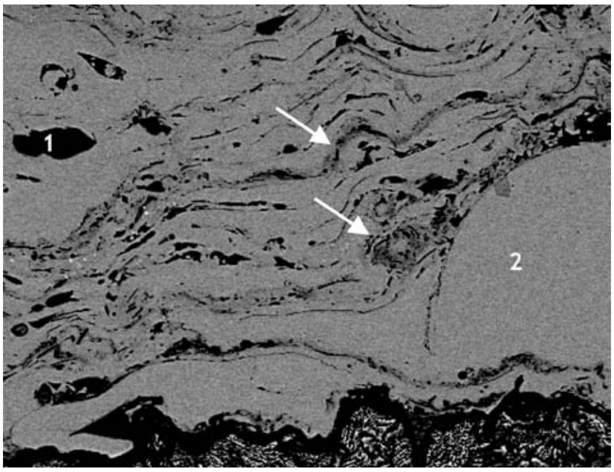

Figure 3 Characteristic features of as-sprayed coating [Back scattered electron image of A2 coating].

observed. As the oxygen flow rate was increased, the amorphous phase fraction was firstly increased and then sharply decreased. Further, the oxide content was measured using EDS on the cross section of coating. A general increase of oxygen content with the increase of O_2/H_2 ratio was observed and a sharp increase at 0.20 O_2/H_2 ratio was noted. From the oxygen content and cross sectional morphology (Fig. 2), the amorphous fraction was largely dependent on the in-flight particle oxidation.

According to O_2/H_2 ratio, thermal properties of as-sprayed coating were measured using DSC. Glass transition temperature and crystallization temperature can be seen in Fig. 6. Glass formabilities of A1, A2, and A3 coating were apparently improved when they were compared with that of feedstock; Tx and Tg of feedstock were all higher than those of coatings. For the glass transition temperature, it decreased linearly with the increase of O_2/H_2 ratio while the crystallization temperature was maximized at A2 coating that was still below the crystallization temperature of feedstock. However, these apparent improvements in glass formabilities of as-sprayed coatings can not be considered to be real improvements. They mainly resulted from the inhomogeneity in chemical composition of as-sprayed coating. During flight, particle oxidation changed the chemistry of the remaining molten droplet. Thus, the amorphous splats must have a wide range of chemical composition and the change of chemistry implies the difference of packing density that is very important in glass formability from the phenomenological viewpoint. Resultantly, the glass formability of each amorphous splat shows different thermal properties. As a matter of fact, chemistry dependent glass formability can be seen in ref. [9].

4. Discussion

HVOF sprayed NiTiZrSiSn bulk amorphous coatings were produced with the change of O_2/H_2 ratio below the stoichiometric composition. Through the previous results, it could be confirmed that the bulk amorphous coating formation was primarily dependent on the in-flight particle oxidation. Again, the oxidation was affected by the flame characteristics. As the oxygen flow rate is increased at the constant hydrogen gas flow rate, the flame temperature is increased due to the enhanced combustion and the partial pressure of oxygen molecule is also increased. That is to say, oxygen to fuel gas ratios have critical roles in the flame gas enthalpy and environment [oxidizing, neutral, or reducing]. According to the gas composition, the gas enthalpy can be calculated by the following equation supposing that the participating oxygen molecules in the gas mixture took

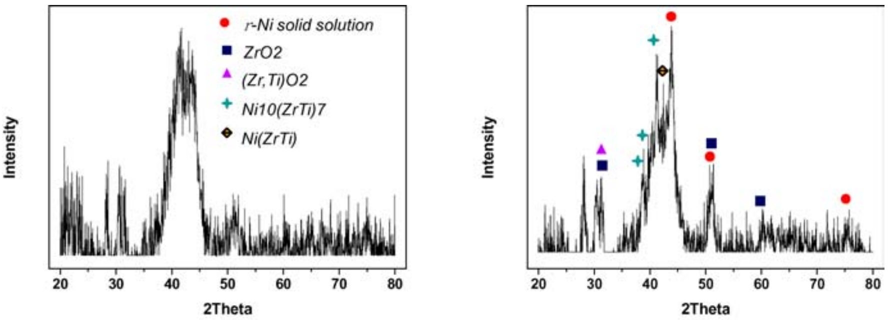

(a) 0.10 O2/H2 ratio

(b) 0.15 O2/H2 ratio

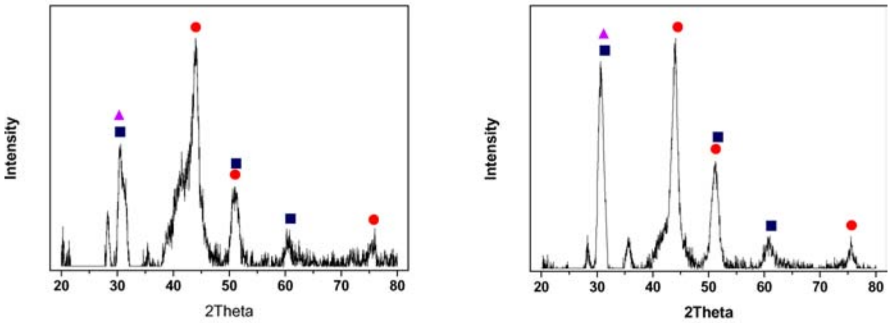

(c) 0.20 O2/H2 ratio

(d) 0.30 O2/H2 ratio

Figure 4 X-ray diffraction of as-sprayed coating according to O_2/H_2 ratio.

part in the combustion.

$$Ht = M_{H_2} \times \Delta H$$

Where Ht is total gas enthalpy, M_{H2} is mole of hydrogen gas per a minute that is combusted, and ΔH is evolved gas enthalpy per mole from $H_2(g) + 1/2O_2(g) = H_2O(g)$ combustion reaction [$\Delta H = -24$ 2kJ]. As O_2/H_2 ratio is increased, the heat of combustion per minute is increased; 1730, 2480, 3170, 4390 kJm^{-1} for 0.1, 0.15, 0.2, and 0.3 respectively. However, it is hard to obtain combustion at 100% efficiency. It means that the free oxygen molecules remain within a flame. The partial pressure of free oxygen can also be expected to increase with the increase of O_2/H_2 ratio. In Table III, the coating properties are summarized. Through the porosity, unmelted particle, and oxygen variation according to O_2/H_2 ratio, flame characteristics effects could be confirmed. In fact, it could be observed that the particle melting state was improved with the O_2/H_2 ratio as shown in Fig. 2; unmelted particle number density decreased with the O_2/H_2 ratio. In addition, the oxygen partial pressure arising from excess oxygen molecules increased with the O_2/H_2 ratio. This makes the flame environment shift from reducing or neutral to oxidizing. This oxidizing environment enhances the in-flight particle oxidation.

In addition to the typical microstructure changes, phase composition of as-sprayed coating varied according to gas composition. The phase evolution could be deduced from the in-flight particle oxidation. When the particle oxidation occurred during flight, it induced the change of chemical composition within a molten droplet. Through the elemental analysis, the oxides produced during the process were zirconium and zirconium/titanium complex oxides. So, the preferential oxidation of Zr and Ti occurred during flight in the hot gas downstream. As the oxidation proceeded, the phase transition occurred in the following sequence.

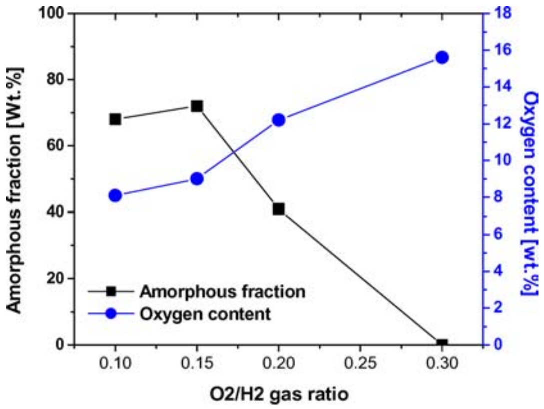

Figure 5 Amorphous phase fraction and oxygen content variations according to the O_2/H_2 ratio.

$$\text{Amorphous} \rightarrow \underset{[\text{Ni(Ti, Zr)and Ni10(Ti,Zr)7}]}{\text{Intermetallic compounds}} \rightarrow \gamma\text{-Ni solid solution}$$

When a pseudo-ternary phase diagram showing the relationship between chemistry and glass formability [ref. *Journal of Non-crystalline Solids*, 2001, 132–136] is considered, the glass formability is different according to chemical composition. There is also a somewhat narrow region for the stabilizing amorphous phase. During HVOF process, Zr and Ti in the particles injected into the flame were oxidized and, resultantly Zr + Ti contents in the remaining liquid were reduced. Thus, the chemical composition of remaining liquid

TABLE III Characterization of coating microstructure according to oxygen to fuel gas ratio

					Participating phase	
Desig	O_2/H_2 ratio	Thickness [μm]	Porosity [Area%]	Oxygen [wt.%]	Major	Minor to trace
A1	0.10	86	2.9	8.1	Amorphous	Intermetallic Oxide
A2	0.15	150	3.3	9.0	Amorphous	Intermetallic Oxide/γ-Ni
A3	0.20	93	0.8	10.4	Amorphous Oxide/γ-Ni	Intermetallic
A4	0.30	84	0.9	13.2	Oxide γ-Ni	Intermetallic Amorphous

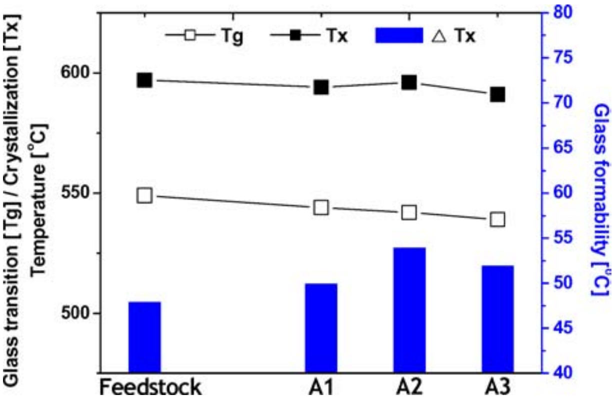

Figure 6 Variation of glass formability of coating according to O_2/H_2 ratio.

was out of the region where amorphous can be stable. For the formation of intermetallic compounds in an as-sprayed coating, it might be due to two different reasons. One is from solid state crystallization of in-flight particles which did not obtain a fully melted state but passed over the crystallization temperature. The other is from the solidification of partially oxidized droplets to intermetallic phases. Changes in chemical composition might have an influence on the critical cooling rate for amorphous formation. As the in-flight particle oxidation is further increased, crystalline phase is shift from intermetallic compound to γ-Ni solid solution besides the increase of oxide and decrease of amorphous phase fraction.

Within the scope of process parameters in this study, fully amorphous coating was not obtained. However, the amorphous-crystalline and amorphous-crystalline-oxide composite coatings could be obtained. It is well known that the amorphous-crystalline composite materials show improved mechanical performance [1, 6, 7]. Therefore, the coating mechanical properties are now evaluated for the as-sprayed coatings. Also, the post spraying heat treatment effects are also investigated considering somewhat wide glass formability of the coating.

5. Conclusion

Through this study, the effect of in-flight particle oxidation on the amorphorization behaviors during solidification in thermal spraying processes was investigated. In the case of HVOF sprayed NiTiZrSiSn coating, the amorphous phase fraction in as-sprayed coating was dependent on the in-flight particle oxidation. Also, the in-flight particle oxidation was increased with the increase of oxygen to fuel gas ratio because oxidation induced destabilization of the amorphous phase.

1. Below the 0.15 O_2/H_2 ratio, crystallization to the intermetallic compounds was observed. This kind of crystallization was partially from the solid-state crystallization of in-flight particle and partially from the increase of chemical destabilization owing to oxidation.
2. Above the 0.20 O_2/H_2 ratio, severe oxidation was observed. The parallel increase of oxide and γ-Ni solid solution fraction was also observed. Considering the unmelted particle fraction, crystallization to γ-Ni solid solution was due to radical increase in destabilization of the impacting particle arising from severe oxidation.
3. Apparent increase of glass formability[ΔTx] was observed with the increase of the O_2/H_2 ratio. It does not imply enhanced glass formability but means the chemical inhomogeneity of impacting particles occurred owing to differences in the oxidation degree particle by particle.

Acknowledgement

We acknowledge that this research was performed using the financial support provided by MOICE (Ministry of Commerce, Industry, and Energy) under the project named development of structural metallic materials and parts with super strength and high performance

References

1. K. KISHITAKE, H. ERA and F. OTSUBO, *J. Ther. Spray Technol.* **5** (1996) 476.
2. A. KAWASHIMA, H. HABAZAKI and K. HASHIMOTO, *Mater. Sci. Engng.* **A304–306**, (2001) 753.
3. X. WANG, I. YOSHII, A. INOUE, Y. H. KIM, I. B. KIM, *Mater. Trans. JIM* **40** (1999) 301.
4. H. J. LEE, E. AKIYAMA, J. JABAZAKI, A. KAWASHIMA, K. ASAMI and K. JASHIMOTO, *Corr. Sci.* **38** (1996) 1269
5. D. T. GAWNE, Z. QIU, T. ZHANG, Y. BAO, K. ZHANG, in Proceedings of the 1st International Thermal Spray Conference (2000) p. 977
6. Thierry Gloriant, *J. Non-Crystalline Solids* **316** (2003) 96.
7. A. L. GREER, *Mater. Sci. Engng.* **A304-306** (2001) 68.
8. J. W. LUSTER, G. R. HEATH and P. A. KAMMER, *Mater. Manufact. Proc.* **115**, (1996) 855.
9. S. YI, J. K. LEE, W. T. KIM and D. H. KIM, *J. Non-Crys. Solids.* **291** (2001) 132.

Received 7 July 2004
and accepted 9 May 2005